

Multi-Parameter ADCs and Memories

Leap over the Barrier to Multi-Parameter Experiments

Incorporating ADCs into a multi-parameter experiment can be a difficult task involving the development of suitable ADCs, computer interfaces, and special software. Typically, the project demands substantial effort from analog and digital electronics engineers, software programmers, and systems engineers. Traditionally, the magnitude of the project has been a significant barrier to implementation.

Now there is a simple solution. CAMAC/FERA bus ADCs from ORTEC and supporting SPARROW Kmax™ Software enable you to leap over the multi-parameter barrier with ease.

Off-the-Shelf, Standard CAMAC ADCs

The ADCs are standard CAMAC modules. This guarantees compatibility with the numerous CAMAC products supplied by other manufacturers. Compatible CAMAC products include crates, power supplies, crate controllers, computer interfaces, and a variety of modular functions. The digital data bus in the CAMAC crate provides computer control and readout for the ADCs. Data transfer rates to a PC up to 1000 ADC data words per second are possible over the CAMAC bus. For applications requiring higher data rates and a large number of parameters, the ADCs offer FERABus readout. The FERABus readout is fully compatible with the LeCroy product line of CAMAC/FERABus modules for fast, multi-parameter data acquisition. Data transfer rates to a PC up to 200,000 ADC data words per second can be accommodated over the FERABus. The availability of standard CAMAC products for interfacing the ORTEC ADCs to a computer eliminates the need for analog and digital electronics engineers.

Standard CAMAC Software, with Ready-to-Run Programs

Kmax Software from SPARROW supports the ORTEC ADCs with ready-to-run programs for the Macintosh® computer, the IBM PC, and IBM-compatible PCs. Standard programs for data acquisition, display, and control are available for 1- to 4-parameter systems. SPARROW can also provide customized programs for more than four parameters, or for any configuration of CAMAC modules you desire. Kmax software offers unprecedented expandability, with Module Description Resource files that support the specific command set of every commercial CAMAC module. For the ORTEC ADCs, Kmax software provides all the features you need for acquiring, sorting, displaying, and analyzing single- or multi-parameter data. With Kmax, you don't need a software programmer.

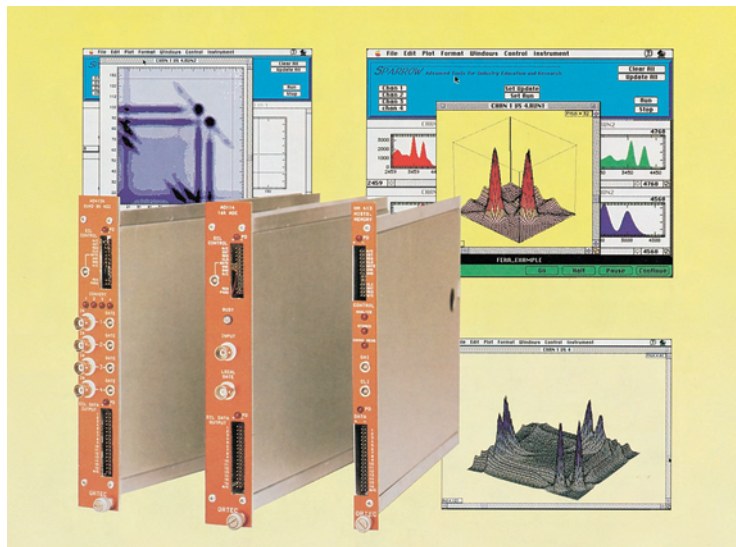
Combining SPARROW software with ORTEC ADCs provides a simple solution for even your most complex multi-parameter requirements.

CAMAC FERABus ADCs from ORTEC are standard products that can be combined with SPARROW Kmax software to build a powerful multi-parameter data collection system. **These ADCs eliminate the need for electronic design engineers.**

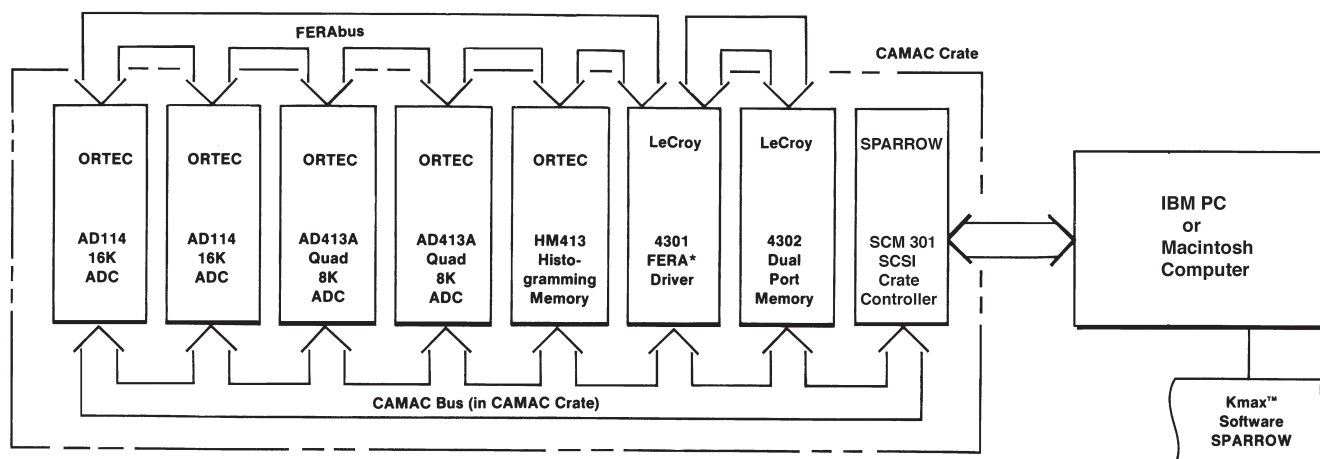
- Fast multi-parameter data collection
- Peak-sensing ADCs with 13- or 14-bit resolution
- Throughput to 100,000 data words per second
- Expandable from 1 to 1024 parameters

Kmax software from SPARROW supports the ORTEC CAMAC ADCs with ready-to-run programs for the Macintosh computer and IBM PCs. **Kmax eliminates the need for software programmers and system engineers.**

- Powerful single- and dual-parameter displays
- Event-by-event data acquisition and sorting
- Unprecedented system expandability (standard package for 1 to 4 parameters; customized solutions available for up to 1024 parameters)
- For details contact www.sparrowcorp.com.



CAMAC ADCs and Memories



The ADC Function

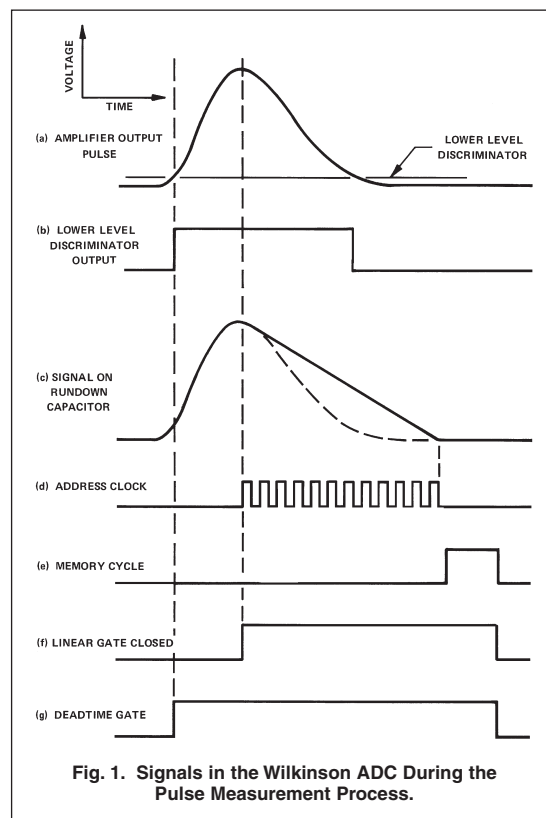
An analog-to-digital converter (ADC) measures the maximum amplitude of an analog pulse and converts that value to a digital number. The digital output is a proportional representation of the analog amplitude at the ADC input. For sequentially arriving pulses, the digital outputs from the ADC are fed to a dedicated memory, or a computer, and sorted into a histogram. This histogram represents the spectrum of input pulse heights. If the input pulses come from an energy spectroscopy amplifier, the histogram corresponds to the energy spectrum observed by the associated detector. When the output of a time-to-amplitude converter is connected to the ADC input, the histogram represents the time spectrum measured by the time-to-amplitude converter. The combination of the ADC, the histogramming memory, and a CRT display of the histogram forms a multichannel analyzer (MCA). If a computer is employed to display the spectrum, then the combination of the ADC and the histogramming memory is called a multichannel buffer (MCB).

ADC Types

Three types of ADCs are available: the flash ADC, the Wilkinson ADC, and the successive-approximation ADC. Only the latter two are used for high-resolution pulse-height spectroscopy.

The Wilkinson ADC

The operation of the Wilkinson ADC is illustrated in Figs. 1 and 2. The lower-level discriminator (Figs. 1a and 1b) is used to recognize the arrival of the amplifier output pulse. Usually, the lower-level discriminator threshold is set just above the noise level to prevent the ADC from spending time analyzing noise. When the input pulse rises above the lower-level discriminator threshold, the input linear gate is open and the rundown capacitor is connected to the input (Fig. 2a). Thus, the capacitor is forced to charge up so that its voltage follows the amplitude of the rising input pulse (Fig. 1c). When the input signal has reached its maximum amplitude and begins to fall (Fig. 1c), the linear gate is closed and the capacitor is disconnected from the input (Fig. 2b). At this point, the voltage on the capacitor is equal to the maximum amplitude of the input pulse. Following peak amplitude detection, a constant current source is connected to the capacitor to cause a linear discharge (rundown) of the capacitor voltage (Figs. 1c and 2b). At the same time, the address clock is connected to the address counter (Figs. 1d and 2b) and the clock pulses are counted for the duration of the capacitor discharge. When the voltage on the capacitor reaches zero, the counting of the clock pulses ceases. Since the time for linear discharge of the capacitor is proportional to the original pulse amplitude, the number N_c recorded in the address counter is also proportional to the pulse amplitude. During the memory cycle (Figs. 1e and 2c), the address N_c is located in the histogramming memory, and one count is added to the contents of that location. The value N_c is usually referred to as "the channel



CAMAC ADCs and Memories

number." ADCs are commonly available with as few as 256 channels for low-resolution applications, and as many as 16,384 channels for high-resolution requirements.

For the Wilkinson ADC, the measurement time of the MCA contributes a non-extending dead time as expressed in Equation (1).

$$T_M = (N_C / f_C) + T_{MC} \quad (1)$$

The MCA dead time depends on the clock frequency f_C , the channel number N_C , and the memory cycle time T_{MC} . Clock frequencies in the range from 50 to 400 MHz are typical, and memory cycle times from 0.5 to 2 μ s are common. As a result, maximum conversion times for an 8192-channel Wilkinson ADC range from 20 to 165 μ s. The advantage of Wilkinson ADCs is low differential nonlinearity (typically <1%). The disadvantage is the long conversion time, which is dependent on pulse amplitude.

The Flash ADC

Figure 3 depicts the principle of the flash ADC. The ADC is constructed by stacking a series of comparators so that each comparator's threshold is a constant increment in voltage ΔV above the previous threshold. The flash ADC is essentially a stack of single-channel pulse-height analyzers with equal window widths and shared thresholds. When the analog input signal is at its maximum amplitude, the outputs of the comparators are strobed into the digital output encoder. The illustration in Fig. 3 is a two-bit (or four-channel) flash ADC. If, for example, the amplitude of the analog pulse falls between the levels of comparators 2 and 3, the binary output code generated is 10 (equivalent to the decimal number 2). The advantage of flash ADCs is speed. Conversion times are in the nanosecond range. The disadvantage is large differential nonlinearity (non-uniformity of channel widths), which generally limits the flash ADC to a resolution of less than eight bits. Because of the large differential nonlinearity and the limited number of bits, the flash ADC is not applicable for high-resolution pulse-height spectroscopy.

The Successive-Approximation ADC

The successive-approximation ADC is illustrated in Fig. 4. During the rise of the analog input pulse, the switch S1 is closed and the voltage on capacitor C1 tracks the rise of the input signal. When the input signal reaches maximum amplitude, S1 is opened, leaving C1 holding the maximum voltage of the input signal. After detection of the peak amplitude of the input pulse, the successive-approximation ADC begins its measurement process. First, the most significant bit of the digital-to-analog converter (DAC) is set. If the comparator determines that the DAC output voltage is greater than the signal amplitude V_s , the most significant bit is reset. If the DAC output voltage is less than V_s , the most significant bit is left in the set condition. Subsequently, the same test is made by adding the next most significant bit. This process is repeated until all bits have been tested. The bit pattern set in the register driving the DAC at the end of the test is a digital representation of the analog input pulse amplitude. This binary number N_C is the address of the memory location to which one count is added to build the histogram representing the pulse-height spectrum. If the ADC has n bits (2^n channels), n test cycles are required to complete the analysis, and this is the same for all pulse amplitudes.

The number of test cycles can be reduced by replacing the single comparator with a flash ADC. For example, in a 16-bit successive-approximation ADC a 6-bit flash ADC is used to determine 5 bits in the first cycle, 5 bits in the second cycle, and the remaining 6 bits in the third cycle. This improves the overall conversion time by reducing the number of cycles from 16 to 3.

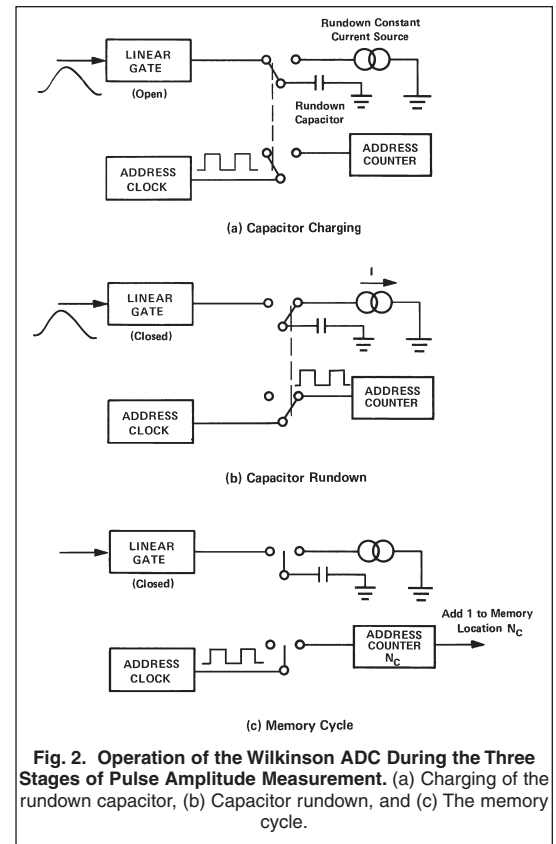


Fig. 2. Operation of the Wilkinson ADC During the Three Stages of Pulse Amplitude Measurement. (a) Charging of the rundown capacitor, (b) Capacitor rundown, and (c) The memory cycle.

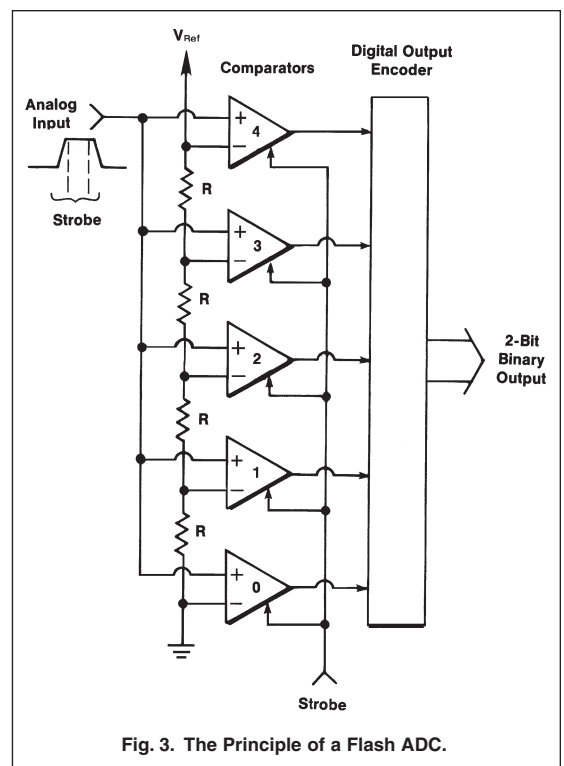
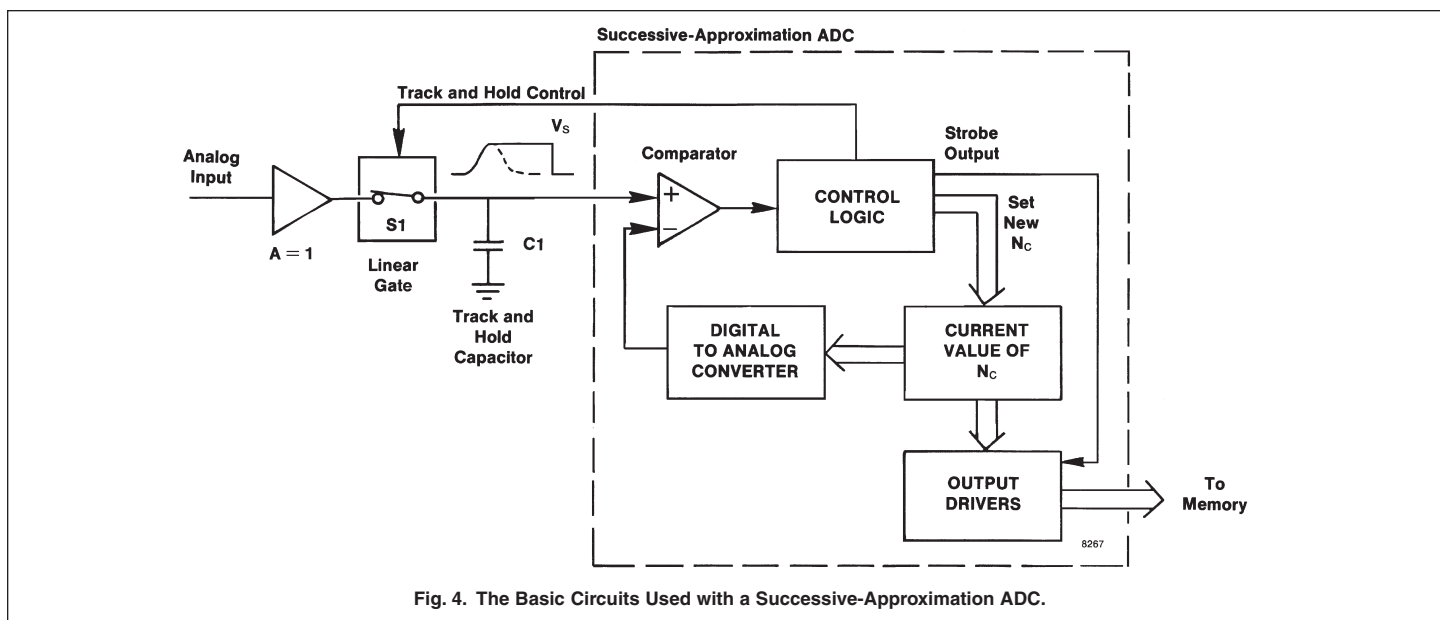


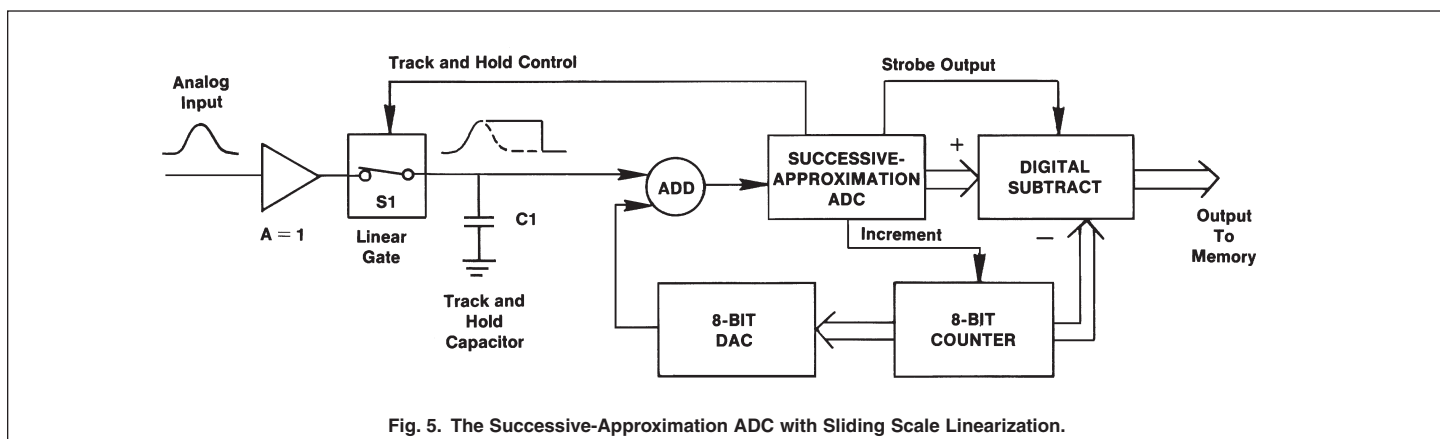
Fig. 3. The Principle of a Flash ADC.

CAMAC ADCs and Memories



Although successive-approximation ADCs are available with the number of bits required for high-resolution spectroscopy, their differential nonlinearity is not adequate. The differential nonlinearity is typically 1/2 of the least significant bit (i.e., 50%). This problem is overcome by adding the sliding scale linearization shown in Fig. 5. After each pulse is analyzed, the 8-bit counter is incremented. This results in an analog voltage being added to the analog input signal before analysis by the successive-approximation ADC. If the number in the 8-bit counter is m , this results in the successive-approximation ADC reporting the analysis m channels higher than normal. By digitally subtracting m at the output of the successive-approximation ADC, the digital representation is brought back to its normal value. As the 8-bit counter increments through its range after each input pulse, it averages the analysis of each pulse height over 256 adjacent channels in the successive-approximation ADC. This reduces the differential nonlinearity to <1%.

The advantages of the successive-approximation ADC with sliding scale linearization are low differential nonlinearity, and a short conversion time that is independent of the pulse amplitude. Conversion times in the range from 2 to 20 μ s are available, with ADC resolutions ranging from 1,000 to 16,000 channels.



CAMAC ADCs and Memories

Input Features

The analog input to the ADC is normally dc-coupled to avoid baseline shifts caused by varying counting rates. A lower-level discriminator is adjustable to prevent analysis of noise, while accepting the lowest possible signal amplitudes. An upper-level discriminator is also employed to prevent the ADC from wasting time converting signals outside the range of allocated memory. This is more important with the longer conversion times, particularly on Wilkinson ADCs.

Typically, logic inputs are provided for coincidence or anti-coincidence gating. The pile-up rejector (PUR) input is a special anticoincidence gate input that is frequently provided to facilitate the use of the pile-up rejector incorporated in many spectroscopy amplifiers. This input permits suppression of the analysis of an analog pulse if a second pulse arrives before the peak amplitude of the first pulse has been detected.

Types of Readout

A variety of readout configurations is available for ADCs that are not inextricably connected to a dedicated memory. ADCs in a NIM package usually offer TTL outputs on a specially defined bus. The CAMAC modular package provides greater flexibility for readout to a computer in larger experiments. It can also offer computer control of the adjustable ADC parameters. For experiments requiring readout of a large number of ADCs with coincident events, the CAMAC package with list-mode readout on the FERAbus is a fast and efficient solution, particularly when zero suppression is employed. The FERAbus readout is able to skip ADCs presenting no information in 3 ns, find the ADCs with active information, and read them out at a rate of 100 ns per word. For example, finding and reading out five nonzero outputs in a 40-input array of ADCs takes about 1.1 μ s.

Dead-Time Effects

When a detector, preamplifier, spectroscopy amplifier, and ADC are combined to form a spectroscopy system, the dead times of the amplifier and the ADC are in series. The combination of the amplifier extending dead time followed by the ADC non-extending dead time T_M yields a throughput described by

$$r_o = \frac{r_i}{\exp [r_i (T_W + T_P)] + r_i [T_M - (T_W - T_P)] U [T_M - (T_W - T_P)]} \quad (2)$$

The rate of events arriving at the detector is r_i , and r_o is the rate of analyzed events at the output of the ADC. T_W is the width of the amplifier pulse at the noise discriminator threshold (Fig. 6). T_P is the time from the start of the amplifier pulse to the point at which the ADC detects peak amplitude and closes the linear gate. $U [T_M - (T_W - T_P)]$ is a unit step function that changes T_M value from 0 to 1 when T_M is greater than $(T_W - T_P)$. For successive-approximation ADCs, T_M is the fixed conversion time of the ADC and includes the time required to transfer the data to the subsequent memory. With a Wilkinson ADC, the value of T_M is given by Eq. 1. At high counting rates, it is desirable to have an ADC conversion time that is less than the time taken for the amplifier pulse to return to the baseline after peak amplitude.

Correction for the dead-time losses implied by Eq. 2 can be accomplished by several methods. Those ORTEC ADCs, MCAs, and MCBs incorporating live-time clocks typically utilize the Gedcke-Hale livetimer.¹ In that case, the livetimer subtracts time during the time interval T_P in order to compensate for pile-up losses. The live-time clock is turned off from the time of peak detection until the pulse returns to baseline $(T_W - T_P)$, or until the ADC dead-time interval T_M is over, whichever interval is longer.

For ADCs without live-time clocks, the scheme in Fig. 7 can be used to correct for dead-time losses. A pulser with a 93- Ω output impedance, a fast rise time, and an adjustable, exponential decay time injects reference pulses into the amplifier input in parallel with the preamplifier output. First, the amplifier pole-zero cancellation is

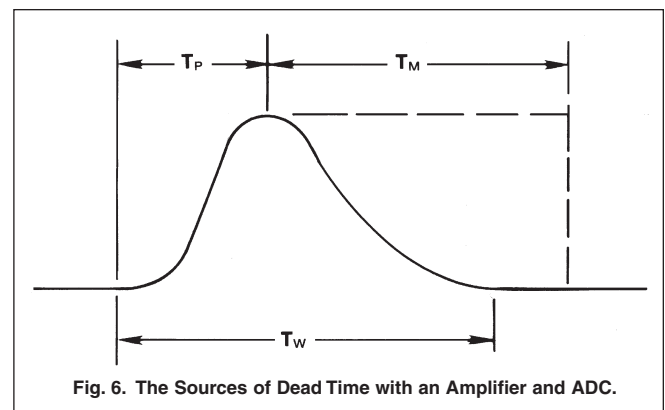


Fig. 6. The Sources of Dead Time with an Amplifier and ADC.

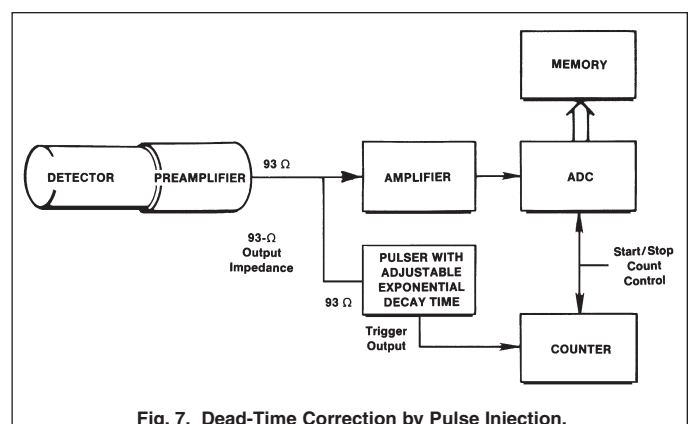


Fig. 7. Dead-Time Correction by Pulse Injection.

CAMAC ADCs and Memories

adjusted on the signals from the preamplifier with the pulser turned off. The amplifier pole-zero adjustment is left in that position for the remainder of the operation. Second, the pulser is turned on, and its decay time is adjusted to achieve perfect pole-zero cancellation on the pulse at the amplifier output. Third, the pulser amplitude is adjusted to place the pulser peak near the high-energy end of the spectrum, where it will not interfere with radiation peaks that must be analyzed. During the measurement time, the ADC will accumulate pulser events in the spectrum, along with real events from the detector. The pulses from the pulser experience the same dead-time effects as do the real events from the detector. If the counter is turned on and off at the same time as the ADC, the number in the counter represents the number of pulses presented to the amplifier by the pulser. The counts in each channel of the spectrum must be multiplied by the ratio of the number in the counter to the number of counts in the spectrum's pulser peak to correct for the dead-time losses.

For pulsed-reset preamplifiers, the exponential-decay-time pulser must be replaced with a low-frequency (<100 Hz) square wave generator, whose output is fed to the preamplifier test input. The rise and fall times of the square wave must be similar to the detector charge collection time.

Counting Statistics with Finite Dead Time

If the amplifier and multichannel analyzer had zero dead time, the statistical variance in the counts recorded in any channel of memory would be $\sigma_q^2 = q$, where q is the number of counts recorded in the channel during a counting time t . However, the dead times in the amplifier and the MCA not only suppress the recorded counts according to equation (2), but they alter the variance as well. Several authors have calculated the effect of the dead time on the variance for systems incorporating a single dead time of either the extending or non-extending type.¹ Although the equation for cascaded dead times is not readily available, the single dead time equations indicate that the variance for the recorded counts can be expected to be less than q . Furthermore, this deviation from $\sigma_q^2 = q$ is highly sensitive to the percent dead time losses.

One way to correct for the dead time losses is to measure the counts, q , recorded in the "real" time t , and use equation 2 to calculate the counts, Q , that would have been observed with zero dead time. (The "real" time is the time measured by a clock that does not turn off during dead time intervals.) Under those circumstances, the statistical variance in the corrected counts calculated via equation (2) will be larger than $\sigma_Q^2 = Q$, and the magnification will escalate with increasing percent dead time.¹ In other words, dead time losses degrade the accuracy of the calculated detector counting rate.

A more practical alternative is to use a live time clock to correct for the dead time losses. An "ideal" live time clock¹ is a clock that a) is turned off for the entire time that the spectrometer is unable to record an event arriving at the detector, and b) records one event for each dead time interval. A live time clock is applicable only to random events uniformly distributed in time (constant counting rate). If the events at the detector obey Poisson statistics, then it can be shown that the variance in the number of events, m , recorded in the live time, t_L , is¹

$$\sigma_m^2 = m \quad (3)$$

The counts at the detector before dead time losses can be calculated as

$$M = \frac{m}{t_L} t \quad (4)$$

or the counting rate at the detector can be computed as

$$r_i = M/t = m/t_L \quad (5)$$

It follows rather simply that the percent standard deviation in r_i , r_o , M or m is given by

$$\begin{aligned} \frac{\sigma_m}{m} \times 100\% &= \frac{100\%}{m^{1/2}} \quad (6) \\ &= \frac{\sigma_M}{M} \times 100\% \\ &= \frac{\sigma_{r_o}}{r_o} \times 100\% \\ &= \frac{\sigma_{r_i}}{r_i} \times 100\% \end{aligned}$$

CAMAC ADCs and Memories

Table 1 summarizes the number of counts required to reach a desired level of precision in measuring the counting rate, r_i .

Equation (3) can also be extended to the sum of the counts over any number of channels in the MCA memory, i.e.,

$$\sigma_N^2 = N = \sum_{i=j}^k m_i \quad (7)$$

where N is the sum of the counts m_i in channels j through k. Reference 1 shows how this variance applies to the subtraction of background under peaks.

| Number of Counts in Live Time t_L | Percent Standard Deviation |
|-------------------------------------|----------------------------|
| 1 | 100% |
| 100 | 10% |
| 10,000 | 1% |
| 1,000,000 | 0.1% |

Linearity

As with spectroscopy amplifiers, the linearity of the ADC's response to input signals is an important performance parameter. Two different linearity specifications are required to define the performance of the ADC: the integral nonlinearity, and the differential nonlinearity.

Figure 8 demonstrates the measurement of an ADC's integral nonlinearity. Using a precision pulser with adequately low nonlinearity, a calibration curve of channel number versus input pulse amplitude is plotted. A straight line is fitted to this calibration curve using a least-squares fitting method. The integral nonlinearity is specified as the maximum deviation ΔC_{max} of the measured calibration curve from the straight line, expressed as a percentage of full scale. It is a measure of the deviation from an ideal, straight-line calibration curve.

The differential nonlinearity specifies the non-uniformity of channel widths. For the measurement, a sliding pulser is injected into the ADC input. As the pulse amplitude slowly slides from 0 to 10 V and back to 0 V in repeated cycles, counts are recorded in all channels. In order to reduce the statistical error, the measurement typically takes at least 10 hours to collect sufficient data. If the channel widths are all equal, the counts recorded in each channel will be identical. The differential nonlinearity is computed as the maximum deviation of the counts, in any of the channels, from the average counts in all the channels, expressed as a percentage of the average counts. This is actually a measure of the maximum deviation of channel width from the average channel width, expressed as a percentage of the average channel width.

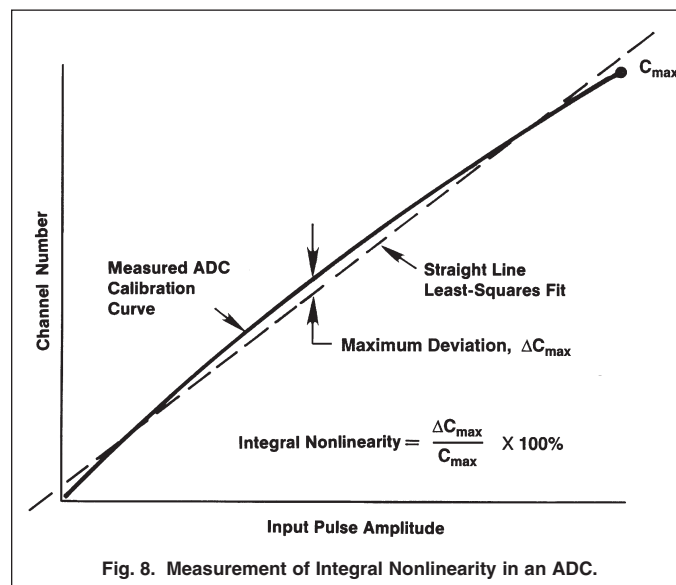


Fig. 8. Measurement of Integral Nonlinearity in an ADC.

¹Ron Jenkins, R.W. Gould, and Dale Gedcke, *Quantitative X-Ray Spectrometry*, (New York and Basel: Marcel Dekker, Inc.,) 1981, pp. 209–287, First Edition.

Specifications subject to change
121709

ORTEC[®]

www.ortec-online.com

Tel. (865) 482-4411 • Fax (865) 483-0396 • ortec.info@ametek.com
801 South Illinois Ave., Oak Ridge, TN 37831-0895 U.S.A.
For International Office Locations, Visit Our Website

AMETEK[®]
ADVANCED MEASUREMENT
TECHNOLOGY